CONCRETE LIBRARY OF JSCE NO.18, DECEMBER 1991

THERMAL DEFORMATION ANALYSIS OF LARGE SCALE STRUCTURES SUBJECTED TO SOLAR RADIATION HEAT

(Abridged Translation from the Proceedings of JSCE, No.420/V-13, Aug. 1990)


Hirotomo YOSHIDA

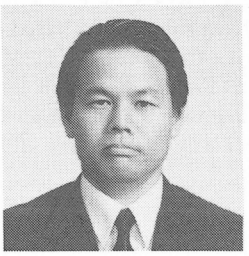
Tada-aki TANABE


Junichiro NIWA

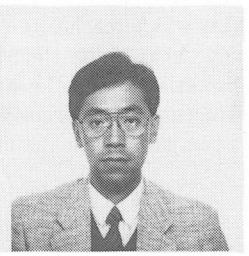
Koji KAYUKAWA

SYNOPSIS

The thermal deformation analysis of a large scale concrete structure subjected to solar radiation heat is carried out. The heat input caused by the solar energy has been formulated considering the shading effect of surrounding obstacles. In the heat transfer analysis, the newly developed shape function has been incorporated into the FEM program. FEM analysis using this shape function can predict measured temperatures of a large scale concrete structure fairly well regardless of considerably rough mesh discretization. Finally the deformation of the structure due to temperatures is calculated and compared with the measured deformation.

H. Yoshida is the president of Nagoya Institute of Technology, Nagoya, Japan. He received his Doctor of Engineering Degree from the University of Tokyo, in 1963. His main research activities are in the area of chemical admixtures for concrete, uses of slag and special cement, and massive concrete. He is a member of JSCE, JCI, and ACI.

T. Tanabe is a professor of civil engineering at Nagoya University, Nagoya, Japan. He received his Doctor of Engineering Degree from the University of Tokyo, in 1971. He is the chairman of JCI committee on the thermal stresses of massive concrete structures. His main research is directed to the dynamic failure mechanism of RC structures. He is a member of JSCE, JCI, IABSE, and ACI.

J. Niwa is an associate professor of civil engineering at Nagoya University, Nagoya, Japan. He received his Doctor of Engineering Degree from the University of Tokyo, in 1983. He specializes in reinforced concrete design and analysis for shear and torsion, application of FEM, and durability design. He is a member of JSCE, JCI, IABSE, and ACI.

K. Kayukawa is a research engineer at Hazama Corporation, Tokyo, Japan. He received his Master of Engineering Degree from Nagoya University, in 1990. His research interests include structural analysis of reinforced concrete. He is a member of JSCE and JCI.

---

1. INTRODUCTION

In order to identify the existing stiffness of a structure, the utilization of thermal deformation is considered as one of the most effective methods [1-3]. In this method, the measured values for the thermal deformation of the structure generated by solar radiation heat is compared with the values obtained by numerical analysis. As a result of checking whether the measured values agree with the analyzed values, the existing stiffness of each section of the structure can be identified. In this study, a large scale concrete structure is selected as the object. First of all, the solar radiation heat which reaches the structure concerned has been calculated. Based on the obtained solar radiation heat, finite element heat transfer analysis is carried out. In FEM, considerably rough mesh discretization for the structure has been employed. Finally, the thermal deformation analysis of the structure is performed using the calculated temperature distribution. The analytical deformation is compared with the measured deformation to identify the existing stiffness of the structure.

2. CALCULATION OF SOLAR RADIATION HEAT [4]

2.1 The Calculation Procedure for Solar Radiation Heat

In calculating the solar radiation heat, the direction vector of the sun from an arbitrary place and time on the earth is needed. Assuming that the earth's orbit is a complete circle, the relationship between the rectangular coordinates fixed on the earth $\{K^*\}$ and the local coordinates at the observation points $\{N^*\}$ can be obtained, as shown in Fig.1.

$$\{K^*\} = [\ k_1^*\ \ k_2^*\ \ k_3^*\ ]\{N^*\} = [\eta]\{N^*\} \tag{1}$$

in which, $[\eta]$ is the coordinate transformation matrix [4]. By using this formula, the direction vector of the sun can be determined.

The heat energy that the structure receives can be calculated by using the Eq.(2), where the sum of the direct solar radiation heat P and the indirect solar radiation heat Q is assumed as the theoretical solar energy R.

$$\left.\begin{aligned} P &= I_0 \cdot p^{(1/sinH)} \cdot \{N\}^T \cdot \{k_2^*\} \cdot S \\ Q &= I_{SH} \\ R &= P + Q \end{aligned}\right\} \tag{2}$$

In Eq.(2), I_0 is the radiation constant of the sun, I_{SH} is the indirect solar heat, p is a ratio of permeation of solar beams through the air, $\{N\}$ is the outward normal line, $\{k_2^*\}$ is the direction vector of the sun from an observation point and S is the surface area of the structure.

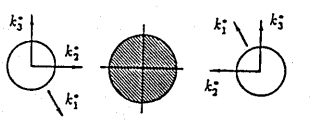

(a) Coordinate on the earth $\{K^*\}$

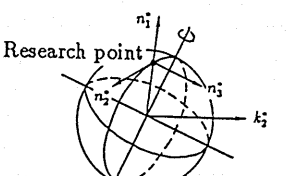

(b) Coordinate on research point $\{N^*\}$

Fig.1 Definition of vector $\{K^*\}, \{N^*\}$

2.2 Numerical Analysis for the Dam and the Result of Solar Energy Calculation

Fig.2 shows the concrete arch dam which is the object of the present analysis, and Fig.3 shows the surrounding topography of this arch dam. The dam is surrounded by mountains, and the upstream dam surface almost faces to the south. Taking the influence of surrounding mountains to the dam into the consideration, the solar energy can be calculated from Eq.(2). Fig.4 shows calculated results of the solar energy obtained on the upstream dam surface (south face) and the downstream dam surface (north face). The change of solar energy generating on the dam surface is shown in Fig.4(a). The solid line in Fig.4(a) shows the change of solar energy with respect of time for the point B' of Fig.2, that is the crest center of the upstream dam surface. Calculated solar energy of points A' and C' near the left and right banks of the upstream dam surface, and points A, B, C of the downstream dam surface exhibits the decrease in the solar energy during certain time periods, because these parts of the dam are shaded by surrounding mountains.

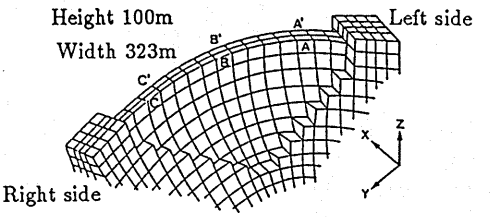

Fig.2 Analysed arch dam

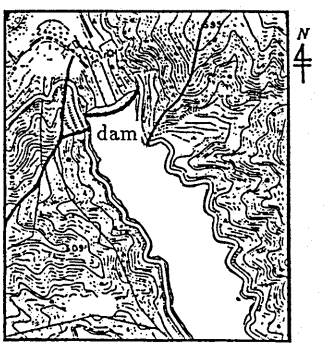

Fig.3 Topography around the arch dam

3. FEM THERMAL ANALYSIS [5]

3.1 Formulation of the Shape Function of the Finite Element

Generally, in the three-dimensional finite element thermal analysis, an eight-node isoparametric hexahedron element is often utilized. However, in the analysis of thin structures such as arch dams, which is taken as the object of this study, it is needed to use very flat element shapes, and therefore, an ordinary linear shape function cannot provide the sufficient accuracy for the prediction of temperatures in the direction of the thickness of the structure. For this reason, we decide to use the exact solution of one-dimensional heat transfer equation as the shape function for FEM.

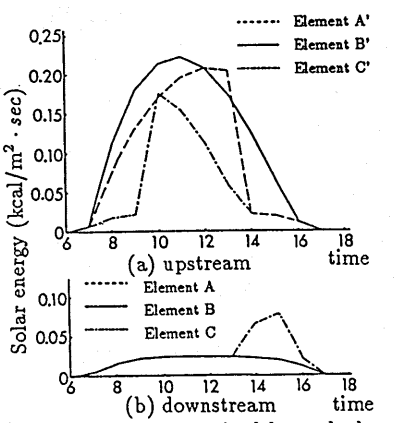

Fig.4 Solar energy received by each element

This shape function is applied only for the direction of thickness of the arch dam, and for another two directions the ordinary linear shape function has been applied. The outline of FEM is as follows. Eq.(3) is the one-dimensional heat transfer equation.

$$\frac{\partial \phi}{\partial t} = \kappa \frac{\partial^2 \phi}{\partial x^2} \quad (\kappa^2 = \frac{K_x}{\rho C} : \text{Heat diffusion ratio}) \tag{3}$$

By solving Eq.(3) based on the initial condition $\phi(x,0) = g(x)$ and the boundary conditions $\phi(0,t) = \phi_1, \phi(L,t) = \phi_2$, Eqs. (4) - (8) can be obtained. Where, ϕ is the temperature, K_x is the heat conductivity coefficient, L is the length of the part, ρ is the density, and C is the specific heat.

$$\phi(x,t) = \phi_1 F(x) + \phi_2 G(x) + H(x) \tag{4}$$

$$F(x) = 1 - \frac{x}{L} + \sum_{n=1}^{\infty} (-\frac{2}{n\pi}) \cdot T_n \cdot sin(\frac{n\pi}{2}x) \tag{5}$$

$$G(x) = \frac{x}{L} + \sum_{n=1}^{\infty} (\frac{2}{n\pi}) \cdot (-1)^n \cdot T_n \cdot sin(\frac{n\pi}{2}x) \tag{6}$$

$$H(x) = \sum_{n=1}^{\infty} (\frac{2g(x)}{n\pi}) \cdot \{1 - (-1)^n\} \cdot T_n \cdot sin(\frac{n\pi}{2}x) \tag{7}$$

$$T_n = exp(-\frac{\kappa^2 n^2 \pi^2}{L^2} t) \tag{8}$$

Eq.(4) is the exact solution of the time t, when the boundary conditions ϕ_1 and ϕ_2 and the initial condition $g(x)$ are provided. This exact solution has been used as the shape function of the thermal distribution in the direction of the element thickness. The temperature of an arbitrary point within the element ϕ can be calculated from Eqs.(9)-(14) by using node temperatures ϕ_1 - ϕ_8 .

$$\phi = [N]\{\phi\} + [M]\{H\} \tag{9}$$

$$[M] = [\ M_1\ M_2\ M_3\ M_4\ ] \tag{10}$$

$$\left.\begin{array}{ll} M_1 = (1-\eta)(1+\zeta)/4, & M_2 = (1+\eta)(1+\zeta)/4 \\ M_3 = (1+\eta)(1-\zeta)/4, & M_4 = (1-\eta)(1-\zeta)/4 \end{array}\right\} \tag{11}$$

$$[N] = [\ N_1\ N_2\ N_3\ N_4\ N_5\ N_6\ N_7\ N_8\ ] \tag{12}$$

$$\left.\begin{array}{ll} N_1 = (1-\eta)(1+\zeta)G(\xi)/4, & N_2 = (1+\eta)(1+\zeta)G(\xi)/4 \\ N_3 = (1+\eta)(1-\zeta)G(\xi)/4, & N_4 = (1-\eta)(1-\zeta)G(\xi)/4 \\ N_5 = (1-\eta)(1+\zeta)F(\xi)/4, & N_6 = (1+\eta)(1+\zeta)F(\xi)/4 \\ N_7 = (1+\eta)(1-\zeta)F(\xi)/4, & N_8 = (1-\eta)(1-\zeta)F(\xi)/4 \end{array}\right\} \tag{13}$$

$$\{H\} = [\ H_1(\xi)\ H_2(\xi)\ H_3(\xi)\ H_4(\xi)\ ]^T \tag{14}$$

3.2 Formulation of FEM Heat Transfer Analysis

The functional χ of the three-dimensional heat transfer equation is expressed by

$$\chi = \int_V \left[\frac{1}{2}\left\{K_x\left(\frac{\partial\phi}{\partial x}\right)^2 + K_y\left(\frac{\partial\phi}{\partial y}\right)^2 + K_z\left(\frac{\partial\phi}{\partial z}\right)^2\right\} + \rho C\frac{\partial\phi}{\partial t}\phi\right]dV + \int_S q\phi dS + \frac{1}{2}\int_S \alpha(\phi-\phi_0)^2 dS \quad (15)$$

where, ϕ is the temperature, K_x - K_z are the heat conductivity coefficients, ρ is the density, C is the specific heat, q is the solar energy, α is the heat transfer ratio, and t is the time. For this functional χ, the temperature ϕ is substituted to obtain the variation of χ. Based on the stationary principle, the finite element equation as shown in Eq.(16) can be obtained.

$$\frac{\partial\chi}{\partial\{\phi\}} = [\tilde{P}]\{\frac{\partial\phi}{\partial t}\} + [\tilde{H}]\{\phi\} + \{\tilde{F}\} = 0 \quad (16)$$

where,

$$\text{Heat Conduction Matrix } [\tilde{P}] = \int_V \rho C[N]^T[N]dV \quad (17)$$

$$\text{Heat Capacity Matrix } [\tilde{H}] = \int_V [B]^T[D][B]dV + \int_S \alpha[N]^T[N]dS \quad (18)$$

$$\text{Load Vector } \{\tilde{F}\} = \int_S q[N]^T dS - \int_S \alpha\phi_0[N]^T dS + \int_V [B]^T[D][DH]^T[M]^T dV + \int_V [B]^T[D][DM]\{H\}dV + \int_S \alpha[N]^T[M]\{H\}dS \quad (19)$$

4. TEMPERATURE DISTRIBUTION OF CONCRETE ARCH DAM

Table.1 Material parameters of concrete and rock [1]

	Concrete	Rock
Heat conductivity coefficient ($kcal/m \cdot sec \cdot ^\circ C$)	0.611×10^{-3}	0.538×10^{-3}
Heat transfer ratio ($kcal/m^2 \cdot sec \cdot ^\circ C$)	0.278×10^{-2}	0.278×10^{-2}
Specific heat ($kcal/g \cdot ^\circ C$)	0.28	0.25
Density (t/m^3)	2.35	2.60

Table.2 Young's modulus and Poisson's ratio of concrete and rock [1]

		Young's modelus (kgf/cm^2)	Poisson's ratio
Rock		5.0×10^4	0.17
Concrete	Water gate	1.0×10^3	
	The others	2.0×10^5	

Using the heat input, that is the solar energy calculated from Eq.(2), and also the measured atmospheric temperature, finite element heat transfer analysis has been performed. Obtained results are shown in Fig.5, and the physical properties of concrete and rocks employed in the analysis are shown in Table 1. Besides the calculated time history of surface temperatures of the typical elements shown in Fig.2, the measured time history of surface temperature and atmospheric temperature at the center part of the dam are also plotted in Fig.5.

The analytical time history of temperature for the element B' on the center part of the upstream dam surface, which receives solar beams directly almost during the daytime, follows the measured temperature accurately. The maximum measured surface temperature is approximately $28°C$, and the calculated value is almost same. The element C' of the upstream dam surface near the right bank exhibits the delayed increase in the temperature compared with the element A' near the left bank and the element B'. The reason why we have such a result is that the part of this arch dam near the right bank is substantially shaded by surrounding mountains in the morning. As for the downstream surface, which does not receive the solar radiation heat almost throughout the day, the analytical temperature exhibits the change in accordance with the change of the atmospheric temperature.

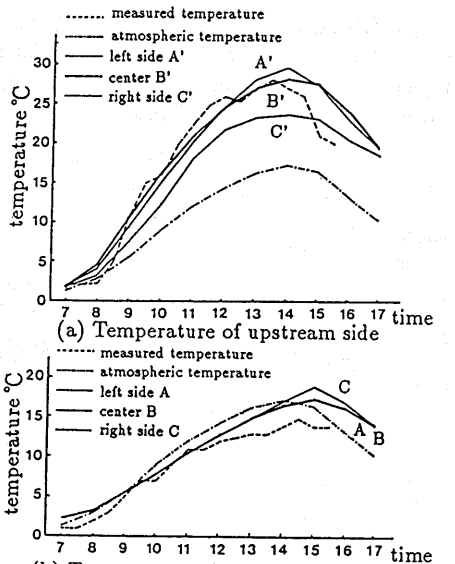

(a) Temperature of upstream side
(b) Temperature of downstream side
Fig.5 Result of thermal analysis

5. THERMAL DEFORMATION ANALYSIS OF CONCRETE ARCH DAM

Based on the results obtained from the analysis for daily temperature change of the dam, the thermal deformation analysis has been carried out. Obtained results are shown in Fig.6. In this deformation analysis, the Young's modulus for the watergate part of the dam has been assumed to be smaller than another concrete portions as shown in Table 2. Predicted horizontal deformation looks like such a mode that a hinge would be formed at the dam center.

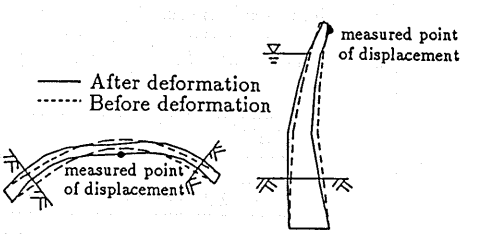

(a) A horizontal plane (b) A vertical plane
Fig.6 Deformation mode of dam

The horizontal displacement at the dam center was measured, and the maximum value was reported to be approximately 1cm [3]. The direction of predicted deformation is similar to the measured direction. However, regarding the absolute value of displacement, the maximum analytical displacement is almost 2.2mm. This difference could be caused from the assumption for the boundary condition on the connection of concrete and rocks in the thermal deformation analysis.

6. CONCLUSIONS

Thermal deformation analysis of a large scale concrete structure has been carried out to evaluate the soundness of the existing concrete structure. Obtained conclusions are as follows:

(1) Based on the exact solution of the one-dimensional heat transfer equation, the temperature distribution of the entire structure can be properly evaluated even with smaller numbers of element discretization.
(2) As for the thermal deformation analysis, the result on the absolute value is still not sufficient. However, the predicted deformation mode is considered to be adequate. To get the proper value for the displacement, and to evaluate the existing stiffness and the soundness of concrete structures, more work is needed. This study is the first step to accomplish this final aim.

REFERENCES

[1] Yoshida,H.,et al. Study on Control System for Large Scale Structure by Laser Beam Sensor, Grant-in Aids for Scientific Research No.58850101,1986

[2] Yoshida, H. , et al. Development of the System to Measure Three-Dimensional Deflection of Structures Using a Laser Diode and a Quadrant Pin Photo Diode, Proceeding OF JSCE No.397 1988

[3] Yoshida,H.,et al. A Study on Deformational Behavior of Concrete Arch Dam to Solar Heat in A Day, Proceeding OF JSCE No.420 1990

[4] Tanabe,T.,et al. Thermal Stress Analysis on The External Cover Wall for 2nd Fireplace at Igata Nuclear Power Station by Solar Energy, Central Research Institute of Electric Power Industry, No.379039, 1982

[5] Larry J. Segerlind, Applied Finite Element Analysis, John Wiley & sons,inc 1976